

Explored An Effective Methodology for Fine-Grained Snake Recognition

Yong Huang¹, Aderon Huang², Wei Zhu³, Yanming Fang⁴ and Jinghua Feng⁵

Huazhong University of Science and Technology, Wuhan, 430074, China

Alibaba Group, Ant Group, MyBank, Hangzhou, 310013, China

Abstract

Fine-Grained Visual Classification (FGVC) is a longstanding and fundamental problem in computer vision and pattern recognition, and underpins a diverse set of real-world applications. This paper describes our contribution at SnakeCLEF2022 with FGVC. Firstly, we design a strong multimodal backbone to utilize various meta-information to assist in fine-grained identification. Secondly, we provide new loss functions to solve the long tail distribution with dataset. Then, in order to take full advantage of unlabeled datasets, we use self-supervised learning and supervised learning joint training to provide pre-trained model. Moreover, some effective data process tricks also are considered in our experiments. Last but not least, fine-tuned in downstream task with hard mining, ensembled kinds of model performance. Extensive experiments demonstrate that our method can effectively improve the performance of fine-grained recognition. Our method can achieve a macro $f1$ score 92.7% and 89.4% on private and public dataset, respectively, which is the 1st place among the participants on private leaderboard. The code will be made available at https://github.com/AderonHuang/fgvc9_snakeclef2022.

Keywords

Fine-Grained Visual Classification (FGVC), Multimodal Backbone, Long Tail Distribution, Self-Supervised Learning (SSL), Hard-Mining

1. Introduction

The human visual system is naturally capable of fine-grained image reasoning, likely it not only distinguishes a dog from a wolf, but also know the difference between a Sea Snake and a Land Snake. Fine-grained visual classification (FGVC) was introduced to the academic community for the very same purpose, to teach how to “see” with machine in a fine-grained manner. FGVC approaches are present in a wide-range of applications in both industry and research, with examples including automatic biodiversity monitoring, improving eco-epidemiological data [1, 2, 3], and have resulted in a positive impact in area such as conservation [4] and commerce [5].

Fine-grained visual classification (FGVC) focuses on dealing with objects belonging to multiple subordinate categories of the same meta-category (e.g., different species of snakes or different models of sorghums). As illustrated in Figure 1, fine-grained analysis lies in the continuum

CLEF 2022: Conference and Labs of the Evaluation Forum, September 5–8, 2022, Bologna, Italy

✉ yonghuang.hust@gmail.com (Y. Huang); xugan.hy@alibaba-inc.com (A. Huang); wei.wz@antgroup.com

(W. Zhu); yanming.fym@antgroup.com (Y. Fang); jinghua.fengjh@alibaba-inc.com (J. Feng)

🌐 <https://github.com/AderonHuang> (A. Huang)



© 2022 Copyright for this paper by its authors. Use permitted under Creative Commons License Attribution 4.0 International (CC BY 4.0).

CEUR Workshop Proceedings (CEUR-WS.org)

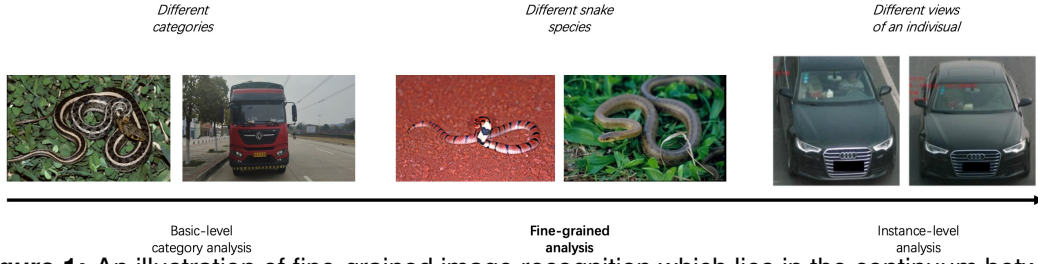


Figure 1: An illustration of fine-grained image recognition which lies in the continuum between the basic-level category analysis (i.e., generic image analysis) and the instance-level analysis.

between basic-level category analysis (i.e., generic image analysis) and instance-level analysis (e.g., the identification of individuals). Particularly, what differs FGVC from generic image analysis is that target objects be classified to coarse-grain meta-categories in generic image analysis and thus are significantly different (e.g., determining if an image contains a bird, a fruit, or a dog). However, in FGVC, since objects typically come from subcategories of the same meta-category, the fine-grained nature of the problem causes them to be visually similar [6]. As an example of FGVC task, in Figure 2, the task is to classify different species of snakes. For accurate image recognition, it is necessary to capture the subtle visual differences (e.g., discriminative features such as length, body shape or body color). Furthermore, as noted earlier, the fine-grained nature of the problem is challenging because of the small inter-class variations caused by highly similar sub-categories, and the large intra-class variations in background, scale, rotations. It is such as the opposite of generic image analysis (i.e., the small intra-class variations and the large inter-class variations), and what makes FGVC a unique and challenging problem.

Formule: In generic image recognition, we are given a training dataset $\mathcal{D} = \{(\mathbf{x}^{(n)}, y^{(n)}) \mid i = 1, \dots, N\}$, containing multiple images and associated class labels (i.e., \mathbf{x}

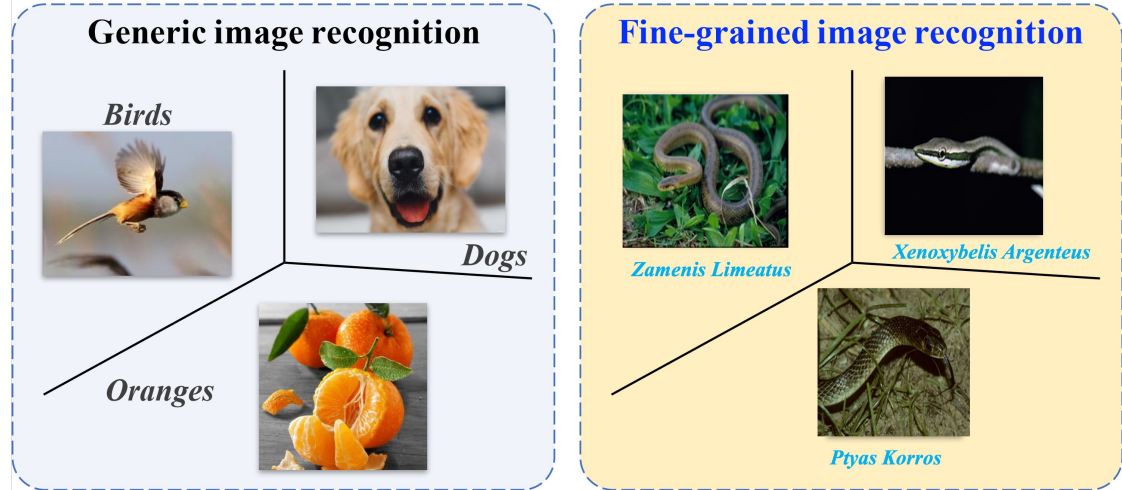


Figure 2: Generic image analysis vs fine-grained image recognition (using visual classification as an example).

and y), where $y \in [1, \dots, C]$. Each instance (\mathbf{x}, y) belongs to the joint space of both the image and label spaces (*i.e.*, \mathcal{X} and \mathcal{Y} , respectively), according to the distribution of $p_r(\mathbf{x}, y)$

$$(\mathbf{x}, y) \in \mathcal{X} \times \mathcal{Y}. \quad (1)$$

In particular, the label space \mathcal{Y} is the union space of all the C subspaces corresponding to the C categories, *i.e.*, $\mathcal{Y} = \mathcal{Y}_1 \cup \mathcal{Y}_2 \cup \dots \cup \mathcal{Y}_c \cup \dots \cup \mathcal{Y}_C$. Then, we can train a predictive/recognition deep network $f(\mathbf{x}; \theta)$ parameterized by θ for generic image recognition by minimizing the expected risk

$$\min_{\theta} \mathbb{E}_{(\mathbf{x}, y) \sim p_r(\mathbf{x}, y)} [\mathcal{L}(y, f(\mathbf{x}; \theta))] , \quad (2)$$

where $\mathcal{L}(\cdot, \cdot)$ is a loss function that measures the match between the true labels and those predicted by $f(\cdot; \theta)$. While, as aforementioned, fine-grained recognition aims to accurately classify instances of different subordinate categories from a certain meta-category, *i.e.*,

$$(\mathbf{x}, y') \in \mathcal{X} \times \mathcal{Y}_c, \quad (3)$$

where y' denotes the fine-grained label and \mathcal{Y}_c represents the label space of class c as the meta-category. Therefore, the optimization objective of fine-grained recognition is as

$$\min_{\theta} \mathbb{E}_{(\mathbf{x}, y') \sim p'_r(\mathbf{x}, y')} [\mathcal{L}(y', f(\mathbf{x}; \theta))] . \quad (4)$$

2. Related Work

The existing Fine-Grained Visual Classification (FGVC) methods can be divided into image only and multi-modality. The former relies entirely on visual information to tackle the problem of fine-grained classification, while the latter tries to take multi-modality data to establish joint representations for incorporating multi-modality information, facilitating finegrained recognition.

Image Only: Fine-Grained Visual Classification (FGVC) methods that only rely on image can be roughly classified into two categories: localization methods [7, 8, 9] and featureencoding methods [10, 11, 12]. Early work [13, 14] used part annotations as supervision to make the network pay attention to the subtle discrepancy between some species and suffers from its expensive annotations. RA-CNN [15] was proposed to zoom in subtle regions, which recursively learns discriminative region attention and region-based feature representation at multiple scales in a mutually reinforced way. MA-CNN [16] designed a multi-attention module where part generation and feature learning can reinforce each other. NTSNet [17] proposed a self-supervision mechanism to localize informative regions without part annotations effectively. Feature-encoding methods are devoted to enriching feature expression capabilities to improve the performance of fine-grained classification. Bilinear CNN [18] was proposed to extract higher-order features, where two feature maps are multiplied using the outer product. HBP [10] further designed a hierarchical framework to do crosslayer bilinear pooling. DBTNet [11] proposed deep bilinear transformation, which takes advantage of semantic information and can obtain bilinear features efficiently. CAP [19] designed context-aware attentional pooling to captures subtle changes in image. TransFG [20] proposed a Part Selection Module to select discriminative image patches

applying vision transformer. Compared with localization methods, feature-encoding methods are difficult to tell us the discriminative regions between different species explicitly.

Multimodality: In order to differentiate between these challenging visual categories, it is helpful to take advantage of additional information, i.e., geolocation, attributes, and text description. Geo-Aware [21] introduced geographic information prior to fine-grained classification and systematically examined a variety of methods using geographic information prior, including post-processing, whitelisting, and feature modulation. Presence-Only [22] also introduced spatio-temporal prior into the network, proving that it can effectively improve the final classification performance. KERL [23] combined rich additional information and deep neural network architecture, which organized rich visual concepts in the form of a knowledge graph. Meanwhile, KERL [23] used a gated graph neural network to propagate node messages through the graph to generate knowledge representation. CVL [24] proposed a two-branch network where one branch learns visual features, one branch learns text features, and finally combines the two parts to obtain the final latent semantic representations. The methods mentioned above are all designed for specific prior information and cannot flexibly adapt to different auxiliary information.

3. Method

Analyze dataset firstly, we introduce the strong multimodal framework, and propose a new loss function to solve long tail distribution with dataset. Then, to make use of enormous unlabeled data, we design a self-supervised leaning framework. It can joint train with supervised learning framework by using joint loss function, as well as completely self-supervise leaning to provide pre-trained model. Furthermore, we also consider hard mining methods to improve the robustness and generalization of model. Last but not least, some tricks are used to improve performance. Eventually, models are ensambled by different ways to achieve maximum performance.

3.1. Dataset

Based on the metadata file presented by the organizers, we concluded that the data at hand is highly imbalanced, which can be considered as the question of long tail distribution. Since this could have negatively influenced our models, we need use weighted loss to counteract this phenomenon. Figure 3 provides an insight for the number to each class in the training set.

3.2. Multimodal Framework

We took MetaFormer [25] and ConvNext [26] as our initial baseline. As shown in Figure 4, MetaFormer is a mixed and multimodal framework that combines ConvNet and Transformer. It supports a simple and effective way for adding meta-information using transformer block. In our approach, we use MetaFormer and modify the input of meta-information, specially, images initially input convolution to encode vision token, and use one-hot encoding to encode attribute meta-information such as location code, country, endemic and temporal binomial name to meta token. Vision token, Class token, Meta token are used for information fusion through the Relative Transformer layer. We also consider ConvNext as another network architecture to enhance the model diversity for later model ensemble, which is a pure ConvNet and strong feature extraction

network. We apply hyperparameter fine-tuning to improve their performance. Some experimental details would illustrate the later ablation studies in Sec 4.

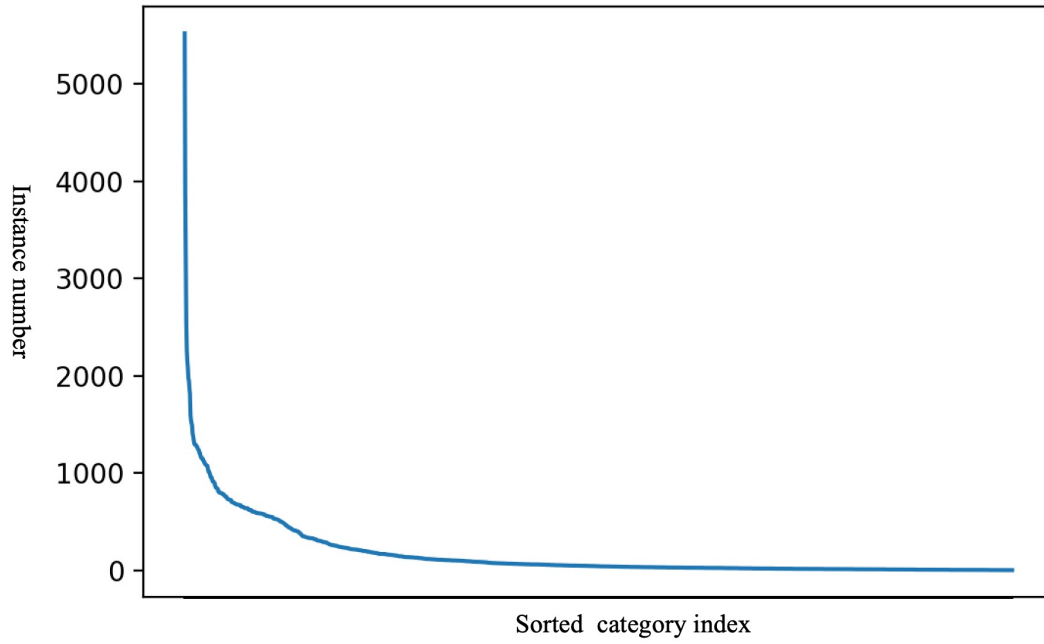


Figure 3: Insight for the number of each class in the training set.

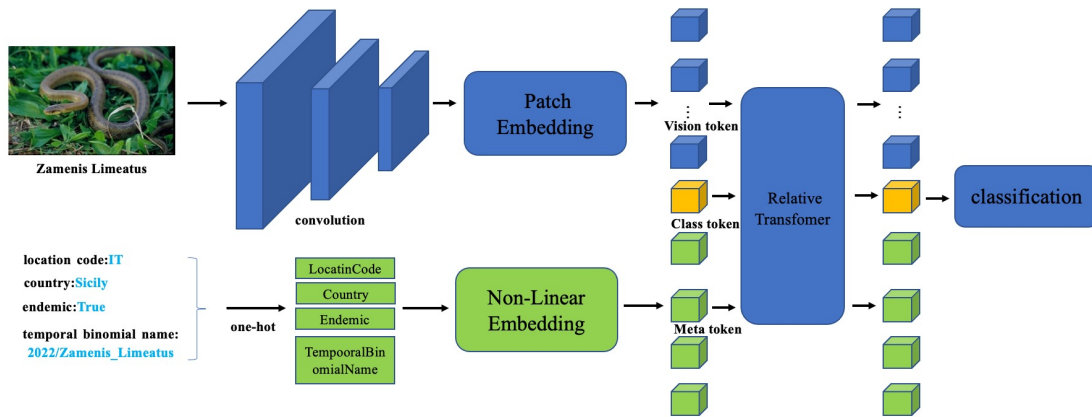


Figure 4: The overall multimodal framework, including visual information and text information.

3.3. Effective Long-Tailed Loss

The classifier trained by the widely applied Cross-Entropy (CE) Loss [27] is highly biased on longtailed datasets, resulting in much lower accuracy of tail classes than head classes. The major reason is that gradients brought by positive samples are overwhelmed by gradients from negative samples in tail classes. We know Arcface Loss [28], Seesaw Loss [29], Polyloss [30], Circle Loss [31], Additive Margin Softmax Loss [32] that are applied to solve long-tailed distribution. We also attempt hard mining method to improve model performance. We experiment these loss functions, later in this section, and detailed these works.

Arcface Loss:The most widely used classification loss function, softmax loss, is presented as following:

$$L_{softmax}(x) = -\frac{1}{N} \sum_{i=1}^N \log \frac{e^{W_{y_i}^T x_i + b_{y_i}}}{\sum_{j=1}^n e^{W_j^T x_i + b_j}}, \quad (5)$$

where $x_i \in \mathbb{R}^d$ denotes the deep feature of the i -th sample, belonging to the y_i -th class. The embedding feature dimension d is set to 512 in this paper. $W_j \in \mathbb{R}^d$ denotes the j -th column of the weight $W \in \mathbb{R}^{d \times n}$ and $b_j \in \mathbb{R}^n$ is the bias term. The batch size and the class number are N and n , respectively. Arcface loss is presented as following [28]:

$$L_{arcface}(\theta) = -\frac{1}{N} \sum_{i=1}^N \log \frac{e^{s(\cos(\theta_{y_i} + m))}}{e^{s(\cos(\theta_{y_i} + m))} + \sum_{j=1, j \neq y_i}^n e^{s \cos \theta_j}} + l_2. \quad (6)$$

where s is a radius of distributed on a hypersphere for learned embedding features, θ_j is the angle between the weight W_j and the feature x_i , m is an additive angular margin penalty between x_i and W_{y_i} to simultaneously enhance the intra-class compactness and inter-class discrepancy, l_2 is also known as the Euclidean norm to avoid overfitting. Our experiments show that arcface loss perform well.

Seesaw Loss:dynamically re-balances positive and negative gradients for each catogory with two complementary factors, i.e., mitigation factor and compensation factor. Seesaw Loss rewrite the Cross Entropy loss as [29]:

$$L_{seesaw}(z) = -\sum_{i=1}^N y_i \log(\hat{\sigma}_i) + l_2, \quad (7)$$

$$\text{with } \hat{\sigma}_i = \frac{e^{z_i}}{\sum_{j \neq i}^N S_{ij} e^{z_j} + e^{z_i}}.$$

where $z = [z_1, z_2, \dots, z_N]$ are predicted logits and $sigma = [\sigma_1, \sigma_2, \dots, \sigma_N]$ are probabilities of the classifier. And $y_i \in \{0, 1\}$, $1 \leq i \leq N$ is the one-hot ground truth label. l_2 is also known as the Euclidean norm to avoid overfitting. Seesaw loss determines S_{ij} by a mitigation factor and a compensation factor, γ is temperature coefficient, as we can see

$$S_{ij} = \gamma * M_{ij} \cdot C_{ij}. \quad (8)$$

i) Mitigation Factor. Seesaw Loss accumulates instance number D_i for each category i at each

iteration in the whole training process. given an instance with positive label i , for another category j , the mitigation factor adjusts the penalty for negative label j the ratio $\frac{D_j}{D_i}$

$$M_{ij} = \begin{cases} 1, & \text{if } D_i \leq D_j \\ \left(\frac{D_j}{D_i}\right)^p, & \text{if } D_i > D_j \end{cases} \quad (9)$$

ii) Compensation factor. this factor compensates the diminished gradient when there is misclassification, *i.e.*, the predicted probability σ_j of negative label j is greater than σ_i . The compensation factor C_{ij} is calculated as

$$C_{ij} = \begin{cases} 1, & \text{if } \sigma_j \leq \sigma_i \\ \left(\frac{\sigma_j}{\sigma_i}\right)^q, & \text{if } \sigma_j > \sigma_i \end{cases} \quad (10)$$

the exponents p and q is hyper-parameters that control the scale, in our experiments, we empirically set $p = 0.8$, $q = 2$, $\gamma = 0.95$, respectively.

3.4. Self-Supervised Learning

We consider unlabel of the test dataset, to fully mine unlabel data information. We use MoCo Method-based and Simclr Method-based to learn more robust and generalizable performance to compensate for the lack of supervised learning.

MoCo Method-based:Pre-trained model through self-supervision learning, and fine-tune model use of labeled data. As common practice (*e.g.*, [33, 34]), we take two crops for each image under random data augmentation. They are encoded by two encoders, f_q and f_k , with output vectors q and k . Intuitively, q behaves like a “query” [33], and the goal of learning is to retrieve the corresponding “key”. This is formulated as minimizing a contrastive loss function [35]. We adopt the form of InfoNCE [36]:

$$\mathcal{L}_q = -\log \frac{\exp(q \cdot k^+ / \tau)}{\exp(q \cdot k^+ / \tau) + \sum_{k^-} \exp(q \cdot k^- / \tau)}. \quad (11)$$

Here k_+ is f_k ’s output on the same image as q , known as q ’s positive sample. The set $\{k^-\}$ consists of f_k ’s outputs from other images, known as q ’s negative samples. τ is a temperature hyper-parameter [37] for ℓ_2 -normalized q , k . We empirically set 0.25 in later experiments. Algorithm 1 show its pseudocode.

Simclr Method-based:It likes to weakly supervised learning, we use unlabeled data and labeled data joint training to provide pre-trained model. Then, we also use labeled data to fine-tune classified head. Its pre-trianed loss can be written as:

$$L_{joint-loss} = \lambda_1 * L_{sup} + \lambda_2 * L_{self-sup}. \quad (12)$$

λ_1 and λ_2 are the supervised and self-supervised learning balance coefficients, respectively, which mainly adjust the balance stability in supervised and self-supervised training, and avoid the phenomenon of separately dominant learning. L_{sup} and $L_{self-sup}$ are supervised loss and self-supervised loss, respectively. We empirically set 0.9 and 0.1 through multiple experiments respectively. Algorithm 2 shows its pseudocode.

Algorithm 1 MoCo Method-based: Pseudocode of in a python-like style.

```
# f_q: encoder representation feature: backbone + proj mlp + pred mlp
# f_k: momentum encoder representation feature: backbone + proj mlp
# m: momentum coefficient
# tau: temperature

for x in loader: # load a minibatch x with N samples
    x1, x2 = aug(x), aug(x) # augmentation
    q1, q2 = f_q(x1), f_q(x2) # queries: [N, C] each
    k1, k2 = f_k(x1), f_k(x2) # keys: [N, C] each

    loss = ctr(q1, k2) + ctr(q2, k1) # symmetrized
    loss.backward()

    update(f_q) # optimizer update: f_q
    f_k = m*f_k + (1-m)*f_q # momentum update: f_k

# contrastive loss
def ctr(q, k):
    logits = mm(q, k.t()) # [N, N] pairs
    labels = range(N) # positives are in diagonal
    loss = CrossEntropyLoss(logits/tau, labels)
    return 2 * tau * loss
```

Algorithm 2 Simclr Method-based: Pseudocode of in a python-like style.

```
# f is network representation, like Metaformer-2,

for x in loader1: # load a unlabeled minibatch x with N samples
    for x_k in x:
        # draw two different augmentation functions, consider as aug1 and aug2
        # the first augmentation
        x_(2k-1) = aug1(x_k)
        h_(2k-1) = f(x_(2k-1)) #representation
        z_(2k-1) = g(h_(2k-1)) #projection

        # the second augmentation
        x_(2k) = aug1(x_k)
        h_(2k) = f(x_(2k)) #representation
        z_(2k) = g(h_(2k)) #projection
    for i, j in zip(z_(2k-1), z_(2k)):
        s(i, j) = z(i)*z(j)/(||z(i)|| ||z(j)||)

    # update networks f and g to minimize loss
    loss_(self-sup) = InfoNCE(s(i, j))

for xx in loader2: #load a labeled minibatch x with N samples
    xx1 = aug(xx)
    h = f(xx1) #representation
    z = g(h) #mlp
    loss_(sup) = CrossEntropy(z)
def ctr(loss_self-sup, loss_sup):
    loss = p * loss_sup + q * loss_self-sup
    return loss
```

3.5. Pre-Post-Process

Pre-Process. Through statistical analysis of the training data, we observed that the foreground is small in the background, far from the center of the image, or there is not foreground. Therefore, in order to ensure that the foreground handles the image center position as much as possible, we use the target detector to crop out the foreground objects in the training set and test set. For images without foreground or images that are missed by the detector, the original scale is retained, and then send to the classifier. We show in Figure 5, original image and cropped image.

Post-Process. We have use center crop, five crop and multi scale ten crop during test phase,

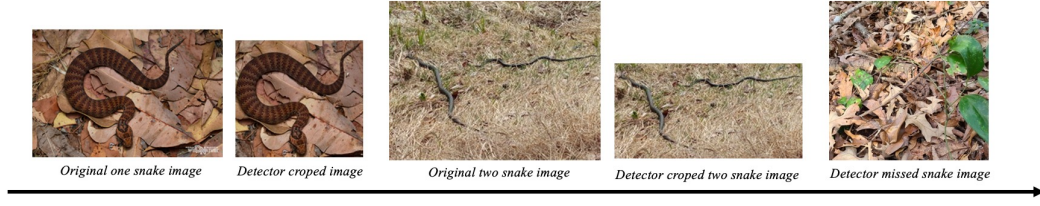


Figure 5: original image, detector cropped image and detector missed image.

the effects of test time augmentation (TTA). It should be noted that the mean $f1$ score on public test set is out of accord with private test set in some experiments, and it is hard to decide which TTA is better only based on public score, in consideration of robustness, we have chosen multi scale five crop based on the public mean $f1$. Some experiments are shown later section. We finally use different models with their logits. It is acknowledged that the tail categories tend to have lower logits compared to head categories, so the tail categories is easier to be misclassified as head categories. As shown in Table 7, with our ensembling for tail categories, the mean $f1$ score improves a lot on private test set.

4. Experiments

In this section, we first elaborate on the implementation and training details. Then we introduce ablation studies on loss functions, self-supervised learning and bag of training settings, which improve our single model’s performance gradually. Then we list some other attempts and their results.

4.1. Implementation Details

We trained the model on SnakeCLEF2022 dataset [38] which contains of 270,251 training images belonging to 1,572 species observed from global wide. The dataset has been divided into train and val set, we use both train and val for training in most settings. We report the results on test set which totally contains 48,280 observations with corresponding images, after removing duplication of observations is 28,431. The test set is divided into two parts. The public set contains 20% of the data, and the private set contains 80% of the data. We conduct all the experiments with Tesla A100 (80G) and Tesla V100 (32G). We use AdamW optimizer with cosine learning scheduler, initialize the learning rate to $5e^{-5}$ and scale it by batch size, we include most of the augmentation and regularization strategies of [39] in training, augmentation strategies include random erasing with probability, regularization strategies like to set empirical coefficients for supervised loss and self-supervised loss.

4.2. Ablation Studies

As show in Table 1, We trained MetaFormer-2 for 300 epochs, with Soft Target Cross Entropy loss and mixup augmentation to build our baseline. For ablation studies, it should be noted that

except the parameter to be compared, there are little other not consistent parameters. such as the accumulate steps in last row in Table 2, we argue that it will not affects the conclusion largely, therefore, we set the default accumulate steps is 2 in our later experiments.

Table 1

MetaFormer-2 baseline.

public mean $f1$	loss	batch size	accumulate steps	epochs	mixup	train+val
0.76450	Soft Target CE	28	2	150	no	no

Table 2

Mean $f1$ score on public test set with different accumulate steps.

public mean $f1$	loss	batch size	accumulate steps	epochs	backbone	train+val
0.76231	Soft Target CE	28	1	150	MetaFormer-2	yes
0.76450	Soft Target CE	28	2	150	MetaFormer-2	yes
0.76562	Soft Target CE	28	4	150	MetaFormer-2	yes
0.76601	Soft Target CE	28	8	150	MetaFormer-2	yes

Network Framework. MetaFormer compared with pure visual information input. In addition to MetaFormer, meanwhile we have tried to train ConvNext with image data. ConvNext’s results are listed in Table 3. The results of ConvNext are inferior to MetaFormer, thus we did not spend a lot of time to tuning it’s hyper-parameters, and we only add ConvNext-large to the model ensemble process.

Table 3

Mean $f1$ score on public test set with different network framework.

public mean $f1$	loss	batch size	epochs	backbone	meta-information
0.75238	Soft Target CE	28	150	MetaFormer-1	no
0.77056	Soft Target CE	28	150	MetaFormer-2	no
0.75563	Soft Target CE	28	150	ConvNext-base	no
0.76601	Soft Target CE	28	150	ConvNext-large	no
0.76763	Soft Target CE	28	150	MetaFormer-1	yes
0.78652	Soft Target CE	28	150	MetaFormer-2	yes

Loss. As shown in Table 4, Label Smoothing Cross Entropy without mixup augmentation converges faster than Soft Target Cross Entropy with mixup augmentation, Seesaw Loss, Arcface Loss which designed for long tail recognition achieves better result on both public and private test set, we also attempt OHEM loss [40] try to possibly alleviate hard samples, a series of experiments show that it’s not more effective.

Self-Supervised Learning. We use MoCo method-base and Simclr method-base to compare, as shown in Table 5, some experiments show that Simclr method-based better than MoCo method-base, we analyzed that self-supervised representation learning joint with supervised learning is

Table 4Mean $f1$ score on public test set with different loss functions.

public mean $f1$	loss	batch size	epochs	backbone	meta-information
0.78652	Soft Target CE	28	150	MetaFormer-2	yes
0.83243	Arcface	28	150	MetaFormer-2	yes
0.82792	Seesaw	28	150	MetaFormer-2	yes
0.80569	Polyloss	28	150	MetaFormer-2	yes
0.81478	Circleloss	28	150	MetaFormer-2	yes
0.82733	AM-softmax	28	150	MetaFormer-2	yes
0.83103	OHEM	28	150	MetaFormer-2	yes

more friendly for downstream tasks, due to the semantic information learned by joint training has synchronized supervised information.

Table 5Mean $f1$ score on public test set with self-supervised learning.

public mean $f1$	loss	image size	epochs	backbone	self-supervised
0.85371	Arcface	384	300	MetaFormer-2	Moco-method-base
0.85734	Arcface	384	300	MetaFormer-2	Simclr-method-base
0.86347	Arcface	512	300	MetaFormer-2	Simclr-method-base
0.86035	Arcface	384crop	300	MetaFormer-2	Simclr-method-base
0.87741	Arcface	384crop+aug	300	MetaFormer-2	Simclr-method-base

Pseudo label. We approximately selected top scores test samples by its logit score, and taken predicted class as their pseudo label. We trained MetaFormer-2 with train+val+pseudo, the results are listed in Table 6.

Table 6Mean $f1$ score on public test set with pseudo label number.

public mean $f1$	loss	image size	epochs	backbone	self-sup	pseudo label
0.87803	Arcface	384	150	MetaFormer-2	yes	+10%
0.88322	Arcface	384	150	MetaFormer-2	yes	+20%
0.88767	Arcface	384	150	MetaFormer-2	yes	+30%
0.88560	Arcface	384	150	MetaFormer-2	yes	+40%
0.88591	Arcface	384	150	MetaFormer-2	yes	+50%
0.86697	Arcface	384	30	MetaFormer-2	yes	+30%
0.90531	Arcface	384	50	MetaFormer-2	yes	+30%
0.90324	Arcface	384	60	MetaFormer-2	yes	+30%
0.89457	Arcface	384	100	MetaFormer-2	yes	+30%

Post Process. As shown in Table 7, we use test time augmentation (TTA) trick in inference, and use final self-supervised Metaformer-2 with 384 image size, totally supervised Metaformer-2

with 384 image size. Meanwhile, combined self-supervised Metaformer-2 with 512 image size and totally supervised Metaformer-2 with 512 image size, also including ConvNext. We finally output fusion models with their highest logit score. It also our final result.

Table 7

Mean $f1$ score on public test set with post process method, including ensemble different models.

public mean $f1$	model	size	crop	TTA	epochs	add pseudo label
0.91324	MetaFormer-2	384	yes	yes	50	yes
0.91872	MetaFormer-2	512	yes	yes	50	yes
0.88356	ssl+ MetaFormer-2	384	no	yes	(300,150)	no
0.89789	ssl+ MetaFormer-2	512	no	yes	(300,150)	no
0.92778	Ensamble					

4.3. Other attempts

Batch Size. Table 8 illustrated that larger batch size improves the performance. in detail, by increasing batch size from 28 to 56, we improved $f1$ score from 0.76450 to 0.77211 on public set.

Table 8

Mean $f1$ score on public test set with different batch size.

public mean $f1$	loss	batch size	accumulate steps	epochs	mixup	train+val
0.76450	Soft Target CE	28	2	32	no	no
0.77211	Soft Target CE	56	2	32	no	no

Training epochs. We found the training epochs is not the more the better, as shown in Table 9, for MetaFormer-2, it is consistent that proper epochs is essential for better result. Following these observations, we fine-tune self-supervised MetaFormer-2 with 300 epochs, and trained supervised MetaFormer-2 with 180 epochs, which saved the training time.

Table 9

Mean $f1$ score on public test set with different training epochs.

public mean $f1$	loss	batch size	accumulate steps	epochs	mixup	train+val
0.72670	Soft Target CE	28	2	50	no	no
0.75891	Soft Target CE	28	2	100	no	no
0.76450	Soft Target CE	28	2	150	no	no
0.76231	Soft Target CE	28	2	200	no	no
0.72882	Soft Target CE	56	2	50	no	no
0.76237	Soft Target CE	56	2	100	no	no
0.76284	Soft Target CE	56	2	150	no	no

Image Size. It is acknowledged that train the model with larger image size improves it’s performance. As there is a trade-off between image size and training flops, we have only tried to train MetaFormer-2 with 512 size, enlarge image size improves mean $f1$ score on private test set.

Pretrain Dataset. We transfer MetaFormer-2 pretrained on different dataset such as imagenet22k and inaturalist21, the results are shown in Table 10. We think various pretrain provide diverse single model, which will enhance the robustness of ensemble model.

Table 10

Mean $f1$ score on public test set with different pre-trained datasets.

public mean $f1$	loss	batch size	accumulate steps	epochs	mixup	pretrain dataset
0.76450	Soft Target CE	28	2	150	no	imagenet22k
0.76292	Soft Target CE	28	2	150	no	inaturalist21

5. Conclusion

In this paper, we have introduced our solution for SnakeCLEF 2022 competition. To solve this challenging fine-grained visual classification, long-tailed distribution problem, we tried many efforts, such as different network framework to achieve more stronger feature extraction, loss function to solve long-tailed distribution and mine hard samples improve the robustness and generalization of model, self-supervised learning method fully mines unlabeled data information, designed special preprocess and post process tricks to improve overall performance. With these endeavours we achieved 1st place among the participants. The experimental results show the progressive process for single model, and the effectiveness of preprocess and post process for tail categories, other attempts also get expected gains. Due to limit of time and resource, more fine-grained experiments require further refinement. Meanwhile, we believe that meta-information is essential for fine-grained recognition tasks in the future. And, multimodal framwork would provide a way to utilize various auxiliary information.

6. Future Work

For future work, firstly, it is valuable to study the method that self-supervised learning to fine-grained visual classification, we know that more and more research institutes and artificial intelligent companies like Google, Meta devoted to self-supervised representation learning recently, the trend of artificial intelligence towards general artificial intelligence, solved the problem of enormous labeled data. Finally, and the problem of distinguishing between tail categories is worth exploring.

Acknowledgments

The authors would like to thank the organizer to offer a pratice and study platform. We also thank Dr Wei Zhu, Dr Yanming Fang for their guidance.

References

- [1] G. Van Horn, S. Branson, R. Farrell, S. Haber, J. Barry, P. Ipeirotis, P. Perona, S. Belongie, Building a bird recognition app and large scale dataset with citizen scientists: The fine print in fine-grained dataset collection, in: Proceedings of the IEEE Conference on Computer Vision and Pattern Recognition, 2015, pp. 595–604.
- [2] G. Van Horn, O. Mac Aodha, Y. Song, Y. Cui, C. Sun, A. Shepard, H. Adam, P. Perona, S. Belongie, The inaturalist species classification and detection dataset, in: Proceedings of the IEEE conference on computer vision and pattern recognition, 2018, pp. 8769–8778.
- [3] G. Van Horn, E. Cole, S. Beery, K. Wilber, S. Belongie, O. Mac Aodha, Benchmarking representation learning for natural world image collections, in: Proceedings of the IEEE/CVF Conference on Computer Vision and Pattern Recognition, 2021, pp. 12884–12893.
- [4] Iccv 2019 workshop on computer vision for wildlife conservation [online], https://openaccess.thecvf.com/ICCV2019_workshops/ICCV2019_CVWC, 2019.
- [5] Y. Wei, S. Tran, S. Xu, B. Kang, M. Springer, Deep learning for retail product recognition: Challenges and techniques, Computational intelligence and neuroscience 2020 (2020).
- [6] X.-S. Wei, Y.-Z. Song, O. Mac Aodha, J. Wu, Y. Peng, J. Tang, J. Yang, S. Belongie, Fine-grained image analysis with deep learning: A survey, IEEE Transactions on Pattern Analysis and Machine Intelligence (2021).
- [7] W. Ge, X. Lin, Y. Yu, Weakly supervised complementary parts models for fine-grained image classification from the bottom up, in: Proceedings of the IEEE/CVF Conference on Computer Vision and Pattern Recognition, 2019, pp. 3034–3043.
- [8] C. Liu, H. Xie, Z.-J. Zha, L. Ma, L. Yu, Y. Zhang, Filtration and distillation: Enhancing region attention for fine-grained visual categorization, in: Proceedings of the AAAI Conference on Artificial Intelligence, volume 34, 2020, pp. 11555–11562.
- [9] H. Zheng, J. Fu, Z.-J. Zha, J. Luo, Looking for the devil in the details: Learning trilinear attention sampling network for fine-grained image recognition, in: Proceedings of the IEEE/CVF Conference on Computer Vision and Pattern Recognition, 2019, pp. 5012–5021.
- [10] C. Yu, X. Zhao, Q. Zheng, P. Zhang, X. You, Hierarchical bilinear pooling for fine-grained visual recognition, in: Proceedings of the European conference on computer vision (ECCV), 2018, pp. 574–589.
- [11] H. Zheng, J. Fu, Z.-J. Zha, J. Luo, Learning deep bilinear transformation for fine-grained image representation, Advances in Neural Information Processing Systems 32 (2019).
- [12] P. Zhuang, Y. Wang, Y. Qiao, Learning attentive pairwise interaction for fine-grained classification, in: Proceedings of the AAAI Conference on Artificial Intelligence, volume 34, 2020, pp. 13130–13137.
- [13] W. Luo, X. Yang, X. Mo, Y. Lu, L. S. Davis, J. Li, J. Yang, S.-N. Lim, Cross-x learning for fine-grained visual categorization, in: Proceedings of the IEEE/CVF International Conference on Computer Vision, 2019, pp. 8242–8251.
- [14] X.-S. Wei, C.-W. Xie, J. Wu, C. Shen, Mask-cnn: Localizing parts and selecting descriptors for fine-grained bird species categorization, Pattern Recognition 76 (2018) 704–714.
- [15] J. Fu, H. Zheng, T. Mei, Look closer to see better: Recurrent attention convolutional neural network for fine-grained image recognition, in: Proceedings of the IEEE conference on computer vision and pattern recognition, 2017, pp. 4438–4446.

- [16] H. Zheng, J. Fu, T. Mei, J. Luo, Learning multi-attention convolutional neural network for fine-grained image recognition, in: Proceedings of the IEEE international conference on computer vision, 2017, pp. 5209–5217.
- [17] Z. Yang, T. Luo, D. Wang, Z. Hu, J. Gao, L. Wang, Learning to navigate for fine-grained classification, in: Proceedings of the European Conference on Computer Vision (ECCV), 2018, pp. 420–435.
- [18] T.-Y. Lin, A. RoyChowdhury, S. Maji, Bilinear cnn models for fine-grained visual recognition, in: Proceedings of the IEEE international conference on computer vision, 2015, pp. 1449–1457.
- [19] A. Behera, Z. Wharton, P. Hewage, A. Bera, Context-aware attentional pooling (cap) for fine-grained visual classification, arXiv preprint arXiv:2101.06635 (2021).
- [20] J. He, J.-N. Chen, S. Liu, A. Kortylewski, C. Yang, Y. Bai, C. Wang, A. Yuille, Transfg: A transformer architecture for fine-grained recognition, arXiv preprint arXiv:2103.07976 (2021).
- [21] G. Chu, B. Potetz, W. Wang, A. Howard, Y. Song, F. Brucher, T. Leung, H. Adam, Geo-aware networks for fine-grained recognition, in: Proceedings of the IEEE/CVF International Conference on Computer Vision Workshops, 2019, pp. 0–0.
- [22] O. Mac Aodha, E. Cole, P. Perona, Presence-only geographical priors for fine-grained image classification, in: Proceedings of the IEEE/CVF International Conference on Computer Vision, 2019, pp. 9596–9606.
- [23] T. Chen, L. Lin, R. Chen, Y. Wu, X. Luo, Knowledge-embedded representation learning for fine-grained image recognition, arXiv preprint arXiv:1807.00505 (2018).
- [24] X. He, Y. Peng, Fine-grained image classification via combining vision and language, in: Proceedings of the IEEE Conference on Computer Vision and Pattern Recognition, 2017, pp. 5994–6002.
- [25] Q. Diao, Y. Jiang, B. Wen, J. Sun, Z. Yuan, Metaformer: A unified meta framework for fine-grained recognition, arXiv preprint arXiv:2203.02751 (2022).
- [26] Z. Liu, H. Mao, C.-Y. Wu, C. Feichtenhofer, T. Darrell, S. Xie, A convnet for the 2020s, in: Proceedings of the IEEE/CVF Conference on Computer Vision and Pattern Recognition, 2022, pp. 11976–11986.
- [27] Z. Qin, D. Kim, T. Gedeon, Rethinking softmax with cross-entropy: Neural network classifier as mutual information estimator, arXiv preprint arXiv:1911.10688 (2019).
- [28] J. Deng, J. Guo, N. Xue, S. Zafeiriou, Arcface: Additive angular margin loss for deep face recognition, in: Proceedings of the IEEE/CVF conference on computer vision and pattern recognition, 2019, pp. 4690–4699.
- [29] J. Wang, W. Zhang, Y. Zang, Y. Cao, J. Pang, T. Gong, K. Chen, Z. Liu, C. C. Loy, D. Lin, Seesaw loss for long-tailed instance segmentation, in: Proceedings of the IEEE/CVF conference on computer vision and pattern recognition, 2021, pp. 9695–9704.
- [30] Z. Leng, M. Tan, C. Liu, E. D. Cubuk, X. Shi, S. Cheng, D. Anguelov, Polyloss: A polynomial expansion perspective of classification loss functions, arXiv preprint arXiv:2204.12511 (2022).
- [31] Y. Sun, C. Cheng, Y. Zhang, C. Zhang, L. Zheng, Z. Wang, Y. Wei, Circle loss: A unified perspective of pair similarity optimization, in: Proceedings of the IEEE/CVF Conference on Computer Vision and Pattern Recognition, 2020, pp. 6398–6407.

- [32] F. Wang, J. Cheng, W. Liu, H. Liu, Additive margin softmax for face verification, *IEEE Signal Processing Letters* 25 (2018) 926–930.
- [33] K. He, H. Fan, Y. Wu, S. Xie, R. Girshick, Momentum contrast for unsupervised visual representation learning, in: *Proceedings of the IEEE/CVF conference on computer vision and pattern recognition*, 2020, pp. 9729–9738.
- [34] M. Chen, A. Radford, R. Child, J. Wu, H. Jun, D. Luan, I. Sutskever, Generative pretraining from pixels, in: *International Conference on Machine Learning*, PMLR, 2020, pp. 1691–1703.
- [35] R. Hadsell, S. Chopra, Y. LeCun, Dimensionality reduction by learning an invariant mapping, in: *2006 IEEE Computer Society Conference on Computer Vision and Pattern Recognition (CVPR'06)*, volume 2, IEEE, 2006, pp. 1735–1742.
- [36] A. Van den Oord, Y. Li, O. Vinyals, Representation learning with contrastive predictive coding, *arXiv e-prints* (2018) arXiv–1807.
- [37] Z. Wu, Y. Xiong, S. X. Yu, D. Lin, Unsupervised feature learning via non-parametric instance discrimination, in: *Proceedings of the IEEE conference on computer vision and pattern recognition*, 2018, pp. 3733–3742.
- [38] Snakeclef2022 [online], <https://sites.google.com/view/fgvc9/competitions/snakeclef2022>, 2022.
- [39] Z. Liu, Y. Lin, Y. Cao, H. Hu, Y. Wei, Z. Zhang, S. Lin, B. Guo, Swin transformer: Hierarchical vision transformer using shifted windows, in: *Proceedings of the IEEE/CVF International Conference on Computer Vision*, 2021, pp. 10012–10022.
- [40] A. Shrivastava, A. Gupta, R. Girshick, Training region-based object detectors with online hard example mining, in: *Proceedings of the IEEE conference on computer vision and pattern recognition*, 2016, pp. 761–769.